

The effect of aspect ratio on toughness in composites

M. R. PIGGOTT

Department of Chemical Engineering and Applied Chemistry, Materials Research Centre, University of Toronto, Toronto, Ontario, Canada

Much information now exists on factors affecting toughness in composites. Theoretical expressions for fracture energy also abound, in response to the many factors that have been identified as contributing to toughness in fibre reinforced materials.

This material is reviewed from the point of view of the effect of aspect ratio on toughness. Expressions relating fracture energy to aspect ratio are derived and compared with experimental data. It is shown that in many cases aspect ratio should be as large as possible. There are a few cases, however, where the aspect ratio should be as close to the critical value as possible.

1. Introduction

A lot of work has been carried out in the last few years on the various factors that contribute to toughness of a fibre-reinforced composite. At least five different interactions have been identified, all of which can, in certain cases, contribute to fracture. In addition there are, of course, effects which will occur in the absence of any interaction, i.e. the matrix fracture surface energy in the absence of fibres, γ_m , and the fracture energy of ductile fibres, γ_{fd} . However, both of these are sometimes affected by the interaction.

Taking the matrix first, it has been observed that small diameter graphite fibres tend to reduce the width of the plastic zone on either side of a crack in ductile metals [1]. This reduces the value of γ_m .

In the case of the very long ductile fibres (cold drawn, low carbon steel), Helfet and Harris [2] have found that when embedded in polymers, the wires behaved as though the matrix were not present; the major part of the work of fracture could be accounted for by taking the area under the force-distance curve for a single fibre and multiplying by the number of fibres fractured. On the other hand, however, ductile steel wires embedded in aluminium were observed to neck at the crack tip [3]. A major part of the fracture energy of the composite was accounted for by the work in the fibres over a distance of only about one diameter on either side of the crack.

Despite this apparent plastic constraint, the fibres were able to contribute a large component to the work of fracture because the plastic strains in the necks achieved high values ($\sim 100\%$).

Turning now to more direct interaction effects, it was early recognized that easy splitting of the matrix parallel to the fibres caused deflection of cracks, and made crack propagation more difficult [4]. (This is particularly noticeable in green wood.) The associated energy will be designated γ_{ms} .

Another interaction, much investigated, is the work of fibre pull-out. With short fibres, a crack can progress across the matrix without breaking the fibres. Instead of breaking they pull out, doing a large amount of work. This is sometimes thought to take place even when initially continuous, but brittle fibres, have been used [5-8]. This term will be designated γ_{rp} .

Smaller amounts of work arise owing to fibre retraction into the matrix after brittle fracture at the crack plane. The elastic energy in the fibre at the instant of rupture, γ_{rp} , is one component [9], and the matrix work as the fibre is being pulled out prior to retraction, γ_{mt} , is another [10-12].

Finally, shearing effects arise when ductile wires cross cracks obliquely. These have been evaluated and the corresponding fracture work calculated approximately by Hing and Groves [13] and by Helfet and Harris [2]. Flexure of the

wires also occurs, but is thought to contribute little work compared with that due to shear [13]. The various factors thought to contribute to the fracture surface energy are listed in Table I.

In most cases, the fracture energy is a maximum if the fibres pullout over a distance equal to half their critical length for reinforcement. At first sight, this would seem to indicate that composites should be made with fibres of the critical length, in order to make the material as tough as possible. However, this would have a serious effect on strength and modulus [14]. Some optimum fibre length thus seems to be required, and this paper attempts to bring together ideas based on fibre fracture, and those based on fibre pull-out, in an attempt to identify the optimum length.

2. Theoretical considerations

The simplest cases arise when fibres cross cracks by the shortest distance. These will be considered first, and after that the additional effects which occur when fibres are oblique will be considered.

2.1. Fibres normal to the crack plane

Continuous perfectly brittle fibres, which fracture at the crack plane, absorb some energy at the interface with the matrix, and thus contribute to the fracture surface energy an amount given by [10]

$$\gamma_{fb} + \gamma_{mf} = 2\gamma_{fb} = \frac{V_1 d \sigma_{fu}^3}{12 E_f \tau_i} \quad (1)$$

where d is the diameter, σ_{fu} the ultimate tensile strength and E_f the modulus of the fibre. τ_i is the interfacial force between fibre and matrix. Short

fibres, all of which have the same length, and pull-out distance, contribute an amount

$$\gamma_{fp} = \frac{1}{12} V_1 d \tau_i s^2 \quad (2)$$

where s is the aspect ratio (length/diameter) of the fibres.

Fibres having aspect ratios greater than the critical value of [14]

$$s_c = \sigma_{fu} / 2\tau_i \quad (3)$$

will not all pull out; instead, some will break, so the above two expressions should be combined.

Consider one face of the crack. Fracturing fibres will contribute an amount of work, for fibres [10], of

$$2U_{fb} = \frac{\pi d^3 \sigma_{fu}^3}{48 \tau_i E_f}$$

(this includes contributions from both γ_{fb} and γ_{mf} , which in this case are identical). Those that pull out will contribute

$$U_{fp} = \frac{1}{2} \pi d \tau_i l^2$$

per fibre, where l is the embedded length. If there are n fibres crossing unit area of crack, then the number embedded to a length lying between l and $l + dl$ is ndl/L where L is the total fibre length. The total fracture work due to combining terms for fibre pull-out and fibre fracture is

$$\gamma_i = \frac{n}{L} \int_{l_c/2}^{L-l_c/2} 2U_{fb} dl + \frac{n}{L} \int_0^{l_c/2} U_{fp} dl$$

which, substituting the expressions for U_{fb} and U_{fp} comes to

$$\gamma_i = \frac{1}{12} V_1 d \tau_i s_c^2 \left\{ \frac{s_c}{s} + \frac{4\sigma_{fu}}{E_f} \left(1 - \frac{s_c}{s} \right) \right\} \quad (4)$$

TABLE I Factors contributing to the work of fracture

	Symbol	Origin	Form of energy dissipation
Fibre internal work	γ_{fb}	Fibre brittle fracture	Stored elastic energy
	γ_{fs}	Fibre bending during pull-out	Plastic flow during bending
	γ_{fd}	Fibre ductile fracture	Plastic flow and necking
Interface work	γ_{mf}	Difference in tensile strains across interface	Frictional sliding or plastic shear in matrix
	γ_{fp}	Fibre pull-out	Frictional sliding or plastic shear in matrix
Interface and matrix work	γ_{ms}	Splitting of matrix parallel to fibres	Matrix surface energy and fibre-matrix bond energy
Matrix internal work	γ_m	Matrix fracture	Matrix surface energy and plastic flow

Now consider fibres which are not perfectly brittle. When $s < s_c$ a proportion of them will have sufficient length embedded on each side of the crack to fracture, and being ductile, contribute some internal work to the fracture energy. The work due to this will be

$$\gamma_f = V_f \gamma_{fd} \left(1 - \frac{s_c}{s} \right). \quad (5)$$

The total fracture surface energy should thus come to

$$\gamma_T = \gamma_i + \gamma_f + (1 - V_f) \gamma_m + \gamma_{ms}. \quad (6)$$

γ_{ms} is the energy absorbed in any splitting of the matrix that may occur. It has been investigated in the case of laminar materials [15], but little work on it appears to have been done with fibres, so it will not be discussed any further.

2.2. Fibres crossing cracks obliquely

Once again, we will first consider fibres that are perfectly brittle, and break as soon as a critical stress, σ_{fu} , occurs at any point on, or in, the fibre. (We are thus taking no account of either the work of fracture of the fibres, or the statistical nature of the flaws that determine the strength of brittle fibres.)

For fibres all parallel, and crossing a crack at an angle ϕ to the crack plane normal, flexure will occur, resulting in an increase in stress on the convex side of the curved fibres, so that they fail at a lower tensile stress, σ_{fm} , where $\sigma_{fm} \approx \sigma_{fu}(1 - A \tan \phi)$. Here A is a constant, proportional to the ratio of fibre ultimate tensile strength to matrix flow stress [16], so long as the matrix does not crumble beneath the concave portion of the curved part of the fibre locus. For $\tan \phi > 1/A$, σ_{fm} is assumed to be zero. The weakening decreases the critical aspect ratio according to the equation

$$s_{c\phi} = s_c(1 - A \tan \phi). \quad (7)$$

The work of fracture is also reduced, since it is proportional to σ_{fm}^3 . Thus

$$\gamma_{fb\phi} = 2\gamma_{fb}(1 - A \tan \phi)^3 (1 + B \tan^2 \phi). \quad (8)$$

Here B is a constant, approximately proportional to the fibre breaking strain, and arises because the fibre, in being flexed, pushes aside some of the surrounding matrix.

Following the same reasoning as before we find that

$$\gamma_{i\phi} = \frac{1}{12} V_f d \tau_i s_{c\phi}^3 \left\{ \frac{1}{s} + \frac{8\tau_i}{E_f} (1 + B \tan^2 \phi) \left(1 - \frac{s_{c\phi}}{s} \right) \right\} \quad (9)$$

For ductile fibres, such weakening due to flexure does not appear to occur. Thus $s_{c\phi} = s_c$. Instead of Equation 8, therefore, we have

$$\gamma_{fb\phi} = 2\gamma_{fb}(1 + B \tan^2 \phi) \quad (8a)$$

and for Equation 9 we have

$$\gamma_{i\phi} = \frac{1}{12} V_f d \tau_i s_c^2 \left\{ \frac{s_c}{s} + \frac{4\sigma_{fu}}{E_f} (1 + B \tan^2 \phi) \left(1 - \frac{s_c}{s} \right) \right\}. \quad (9a)$$

In addition, shear work will be done on ductile fibres that pull out. The expression used by Hing and Groves [13] can be adapted to suit the case where not all fibres pull out. The work done in shearing a single fibre as it pulls out is

$$U_{fs} = \frac{1}{32} \pi d^2 \sigma_f \tan \phi$$

for $\tan \phi < 2$ where σ_f is the tensile flow stress of the fibre or wire. For $\tan \phi > 2$ the fibres will break because they will be unable to withstand the shearing forces.

The number of fibres embedded to a length between l and $l + dl$ is $dn = n dl / (L \cos \phi)$ per unit area, if n is the number of fibres per unit area normal to the fibre direction. These fibres contribute an amount of internal shear work of

$$U_{fs} dn = \frac{n \pi d^2 \sigma_f \sin \phi}{32 L \cos^2 \phi} l dl.$$

The total contribution these fibres make to the fracture surface energy is

$$\gamma_{fs} = \frac{V_f \sigma_f \sin \phi}{8 L \cos^2 \phi} \int_0^{l_c/2} l dl = \frac{V_f \sigma_f d \sin \phi}{64 \cos^2 \phi} \cdot \frac{s_c^2}{s^2}. \quad (10)$$

In addition, there will be the work of fibre fracture,

$$V_f \gamma_{fd} \left(1 - \frac{s_c}{s} \right)$$

as given in Equation 5.

Finally, to propagate a crack in a plane perpendicular to a planar random array of brittle fibres will require an amount of work obtained by integrating Equation 9 with respect to ϕ over the range 0 to $\tan^{-1} 1/A$ and dividing by the range of possible ϕ values, i.e. $\pi/2$. This can be done with sufficient accuracy by using the approximate relation [16]

$(1 - A \tan \phi)^3 (1 + B \tan^2 \phi) \approx (1 - 2.4A \tan \phi)$ where integration is now carried out between 0

and ϕ_1 with $\tan \phi_1 = 1/(2.4A)$. The result obtained is

$$\gamma_{ir} = \frac{1}{12} V_f d \tau_1 s_{cr}^3 \left\{ \frac{1}{s} + \frac{8\tau_1}{E_f} \left(1 - \frac{s_{cr}}{s} \right) \right\} \quad (11)$$

where

$$s_{cr} = \frac{2s_c}{\pi} [\phi_1 + A \ln(\cos \phi_1)]. \quad (12)$$

For ductile fibres, the corresponding equation to be integrated is Equation 9a and the range of angles is 0 to $\tan^{-1} 2$. In addition, Equation 10 should be integrated over the same range. The results are

$$\gamma_{ir} = 0.059 V_f d \tau_1 s_c^2 \left\{ \frac{s_c}{s} + \frac{4\sigma_{fu}}{E_f} (1 + 0.80B) \left(1 - \frac{s_c}{s} \right) \right\} \quad (11a)$$

and

$$\gamma_{fsr} = 0.012 V_f \sigma_f \frac{s_c^2}{s^2}. \quad (13)$$

3. Discussion

3.1. Toughness – aspect ratio diagrams

For convenience, Table II summarizes the main results. Most of the expressions have their maximum values at the critical aspect ratio, $s_c = \sigma_{fu}/(2\tau_1)$, and Fig. 1 illustrates the case for brittle fibres crossing cracks by the shortest distance (Equation 4). The different curves in Fig. 1 show the effect of different fibre breaking

strains, $\epsilon_{fu} = \sigma_{fu}/E_f$. The plots are dimensionless, but the value of γ_{max} can be calculated from the equation

$$\gamma_{max} = \frac{1}{12} V_f d \tau_1 s_c^2 = \frac{1}{24} V_f \sigma_{fu} l_c \quad (14)$$

knowing σ_{fu} , and either the critical failure length, l_c , or the diameter, d , and the interfacial stress τ_1 .

The curves show that the lower the fibre breaking strain, the more important it is to use fibres with the critical aspect ratio. However, it has been found that pull-out effects occur, even when fibres are continuous. This will be discussed later.

When brittle fibres cross cracks obliquely, the curves for fracture surface energy will have the same form as those shown in Fig. 1. The value of aspect ratio for the maximum value of γ will be reduced to $s_{c\phi}$ where

$$s_{c\phi} = s_c(1 - A \tan \phi)$$

and the maximum value of γ will be reduced to

$$\gamma_{\phi max} = \gamma_{max}(1 - A \tan \phi)^2.$$

A somewhat similar reduction in s_c and γ_{max} occurs in the planar random case.

In the ductile fibre case, two additional terms have to be taken into account. Fig. 2 is a dimensionless plot of these factors, together with a plot of Equation 4 for $\epsilon_{fu} = 0.05$ for comparison. The shear term, γ_{fs} , varies with s in much the same way as γ_1 does. (They are exactly the same for $\epsilon_{fu} = 0$.) The fibre ductile fracture

TABLE II Expressions relating aspect ratio (s) to fracture surface energy. V_f omitted from all expressions

Fibre direction	Brittle fibres		Ductile fibres	
	Long	Short	Long	Short
Normal to crack plane	$\frac{1}{12} d \tau_1 s_c^2 \left\{ \frac{s_c}{s} + \frac{4\sigma_{fu}}{E_f} \left(1 - \frac{s_c}{s} \right) \right\}$ $s_c = \sigma_{fu}/2\tau_1$	$\frac{1}{12} d \tau_1 s^2$	Brittle term and $\gamma_{fd} \left(1 - \frac{s_c}{s} \right)$	$\frac{1}{12} d \tau_1 s^2$
At ϕ to crack plane normal	$\frac{1}{12} d \tau_1 s_c^2 \phi \left\{ \frac{1}{s} + \frac{8\tau_1}{E_f} (1 + B \tan^2 \phi) \left(1 + \frac{s_c \phi}{s} \right) \right\}$ $s_{c\phi} = s_c(1 - A \tan \phi)$ $\tan \phi < 1/A$	$\frac{1}{12} d \tau_1 s^2$	$\frac{1}{12} d \tau_1 s_c^2 \left\{ \frac{s_c}{s} + \frac{4\sigma_{fu}}{E_f} (1 + B \tan^2 \phi) \left(1 - \frac{s_c}{s} \right) \right\}$ and $\frac{d\sigma_f \sin \phi}{64 \cos^2 \phi} \frac{s_c^2}{s^2}$ and $\gamma_{fd} \left(1 - \frac{s_c}{s} \right)$ $\tan \phi < 2$	$\frac{1}{12} d \tau_1 s^2$ and $\frac{d\sigma_f \sin \phi}{64 \cos^2 \phi} s$
Planar—random	$\frac{1}{12} d \tau_1 s_{cr}^2 \left\{ \frac{1}{s} + \frac{8\tau_1}{E_f} \left(1 - \frac{s_{cr}}{s} \right) \right\}$ $s_{cr} = \frac{2s_c}{\pi} \{ \phi_1 - A \ln(\cos \phi_1) \}$ $\tan \phi_1 = 1/(2.4A)$	$\frac{1}{12} d \tau_1 s^2$	$0.059 d \tau_1 s_c^2 \left\{ \frac{s_c}{s} + \frac{4\sigma_{fu}}{E_f} (1 + 0.8B) \left(1 - \frac{s_c}{s} \right) \right\}$ and $0.012 d \sigma_f \frac{s_c^2}{s^2}$ and $\gamma_{fd} \left(1 - \frac{s_c}{s} \right)$	$\frac{1}{12} d \tau_1 s^2$ and $0.012 d \sigma_f s$

d = fibre diameter
 E_f = fibre modulus
 σ_{fu} = fibre ultimate strength

τ_1 = interfacial shear stress
 τ_m = matrix shear flow stress

$A \approx 5.5 \tau_f/\sigma_{fu}$
 $B \approx 0.72 \sigma_{tu}/E_f$

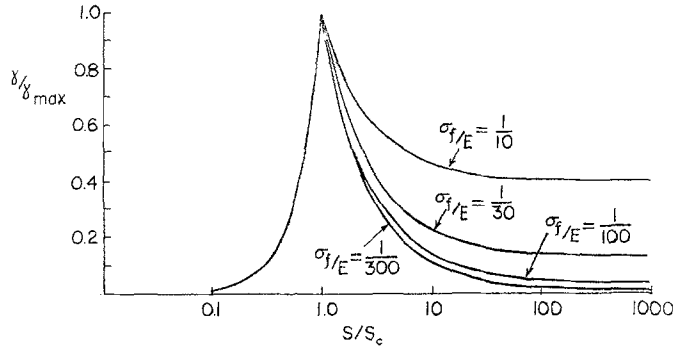


Figure 1 The effect of aspect ratio on toughness for materials reinforced by fibres of uniform strength, negligible internal work of fracture, and various breaking strains. The fibres are normal to the crack plane.

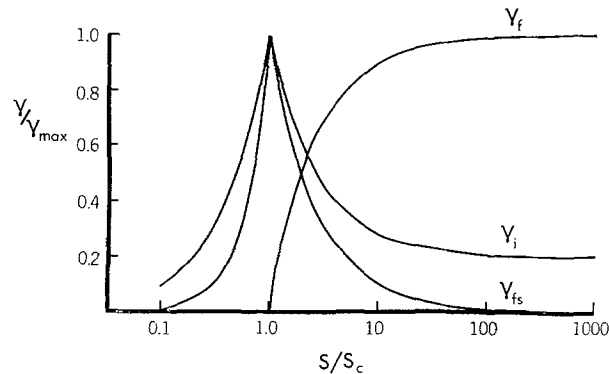


Figure 2 Contributions to fracture energy from shearing fibres (γ_{fs} Equation 10) and fracturing fibres (γ_i Equation 4 and γ_f , Equation 5). The curve is plotted γ_i for $\epsilon_{eu} = 0.05$.

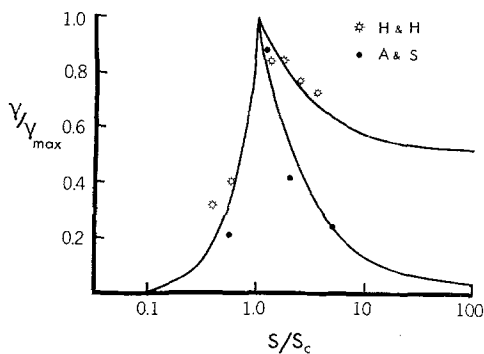


Figure 3 Agreement between the modified model and reported experimental values for work of fracture. The data points for H and H represent the results of Helfet and Harris [2] and those for A and S are from Allred and Schuster [17].

term, however, is zero at the critical length, and tends to a maximum as aspect ratio tends to infinity.

It is clear that with ductile fibres, a wide range of behaviour is possible. To maximize fracture work, two different approaches may be used. Either a large γ_{fs} should be arranged for, by using very long fibres which are very poorly bonded to the matrix, so that they pull out rather than break. Thus γ_{fs} can have high values, and γ_i is also maximized. At the most favourable angle ($\tan \phi \approx 2$), for $\sigma_f \approx \sigma_{fu}$

$$\gamma_{max} = 0.11 V_f \sigma_{fu} l_c \quad (14a)$$

The effect of fibre shear at the most favourable angle is thus to increase the value of γ_{max} by a factor of up to about 2.7 over the highest value for brittle fibres crossing cracks normally.

The alternative approach is to use fibres which have a very high internal work of fracture. They should be well bonded to the matrix, and have an aspect ratio that is at least ten times the critical.

3.2. Comparison with experiment

The expressions described so far represent the ideal behaviour to be expected with flaw-free fibres which interact with the matrix in such a way that, at every point on the fibre surface, the interfacial force has some well-defined value, τ_i . Neither assumption is entirely justified, but two systems have been examined which do, at least, come close to having fibres of uniform strength.

Hellet and Harris [2] embedded steel wires of various lengths in epoxy resins. In the aligned fibre case, the fracture surface energy was observed to have a maximum value when the fibre aspect ratio was about 50. At aspect ratios greater than about 100, the fracture energy appeared to be approaching that due to the work of fracturing free fibres. Using their values for fibre strength, $\sigma_{fu} = 1.20 \text{ GN m}^{-2}$, and critical fibre length, $l_c = 7.5 \text{ mm}$, the maximum toughness should have been

$$\gamma_{\max} = \frac{1}{24} V_f l_c \sigma_{fu} = 37.5 \text{ kJ m}^{-2} \cdot$$

Such a value did not fit their results too well.

This appears to be a case where the assumption of a well-behaved interfacial shear stress, τ_i , needs some modification. It is well known that stress transfer can take place as a result of purely elastic deformation of the matrix, without any slip at the interface [14]. Such stress transfer could be occurring where the stresses and strains in the fibre are small, i.e. near the fibre end in pull-out tests and fracture tests. If the elastic strains can transfer a stress of about 0.5 GN m^{-2} (this requires a bond having a shear strength of about 45 MN m^{-2}), then the value of τ_i over the rest of the fibre length should be only about 7.0 MN m^{-2} .

The presence of end stresses modifies the expression for γ_i , to include a term involving $\sigma_{f0}^3/\sigma_{fu}^3$ (see Piggott [10]) so that Equation 4 becomes

$$\gamma_i = \frac{1}{12} V_f d \tau_i s c^2 \left\{ \frac{s_c}{s} + \frac{4\sigma_{fu}}{E} \left(1 - \frac{\sigma_{f0}^3}{\sigma_{fu}^3} \right) \left(1 - \frac{s_c}{s} \right) \right\} \quad (4a)$$

Using this equation, together with a term for the fracture work of the fibres when not embedded:

$$\gamma_f = V_f \gamma_{fd} \left(1 - \frac{s_c}{s} \right)$$

where $\gamma_{fd} = 114 \text{ kJ m}^{-2}$, we get the result shown in Fig. 3. For $s < s_c$ the equation

$$\gamma = \frac{1}{12} V_f d \tau_i s^2$$

has been used. It will be seen that agreement between the average experimental values and the suggested theoretical curve is reasonably good.

More recently, Allred and Schuster [17] reported some pertinent work on boron fibres embedded in epoxy resin. Their theory did not appear to fit their results, but their results can be fitted into the framework established here. Again we have to assume some elastic stress transfer, so that $\sigma_{f0} \simeq 0.75 \text{ GN m}^{-2}$, requiring a bond able to withstand shear forces of about 55 MN m^{-2} . The value of τ_i comes to only about 4.4 MN m^{-2} compared with the value they assume of 12.2 MN m^{-2} . However, this assumed value was taken from tests [18] on single, larger diameter fibres, embedded in resins subject to tensile stresses. It is quite possible that, in fracture tests, the contraction of the fibre away from the matrix will reduce this interfacial friction stress, compared with its value in the tensile tests, where the matrix is contracting onto the fibre. (Frictional force = μR where R is the normal force and μ is the coefficient of friction; R is likely to be very different in the two cases.) Fig. 3 shows the curve obtained using Equation 4a with s_c having a value of 100 [18].

3.3. Continuous fibres

Materials reinforced with ductile fibres which, when they fracture, dissipate a large amount of internal work (γ_{fd}) will exhibit their maximum work of fracture when the fibres are continuous. In most cases, however, the expressions for fracture surface energy yield relatively low values for continuous fibres, as compared with fibres having the critical length.

Completely brittle continuous fibres crossing cracks normally should have a work of fracture given by Equation 1, i.e.

$$\gamma = \frac{V_f d \sigma_{fu}^3}{12 \tau_i E_f}$$

With large diameter fibres, for example by use of fibre bundles, quite high values for γ can be obtained, despite the fibres being continuous. The results of Fila *et al* [12] for glass-fibre-bundle reinforced polyester resins indicated that values as high as 100 kJ m^{-2} are possible, even for volume fractions as low as about 0.2. Their

results with glass and carbon bundles were in agreement with Equation 1, except that the constant came to about 6, rather than 12. Notched bend tests were used to determine the fracture surface energy.

More recently, Mandell and McGarry [11] have reported the results of tensile compliance tests to measure the fracture energy of carbon and glass-bundle reinforced epoxies and polyesters. They observed the same whitening of the stressed glass-fibre bundles that Fila *et al* did, but interpreted it as indicating debonding, rather than shear flow of material at the interface. τ_1 , calculated from the length of the white region, visible in Mandell and McGarry's Fig. 4, comes to about 38 MN m⁻², compared with 10 to 29 MN m⁻² for Fila *et al*. These values are not too far from the shear failure stress of the matrix, suggesting that some form of matrix shear flow at the interface is not ruled out. Their glass fibre bundle results are in good agreement with Equation 1, despite the difference in testing methods, but as Fila *et al* observed, it appears that the constant should have a value close to 6, rather than 12. This may be because of internal work in the bundles.

Fibre bundles are quite likely to have uniform strength, since the effects of flaws in individual fibres are often swamped by the very large numbers of neighbours not having flaws in the same region. However, in the case of single fibres of carbon and glass, the presence of flaws makes the fibre strength far from uniform. The incorporation of very long pieces of such flawed, single, fibres into matrices sometimes leads to toughening effects which are much greater than to be expected on the basis of Equation 1.

Beaumont and Harris [7] found that γ for carbon-fibre reinforced epoxy resins came to 2.5 to 9 kJ m⁻² instead of 0.07 kJ m⁻² calculated from Equation 1 with τ_1 equal to the minimum value of the interlaminar shear strength (50 MN m⁻²). In addition, pull-out effects were observed. As mentioned earlier, pull-out effects with continuous fibres have also been observed by Phillips [8]; also Sambell *et al* observed pull-out effect with long fibres [19], and they obtained higher fracture energies with continuous fibres than with short ones [20].

These effects may be a consequence of the deformation resulting from the stress concentration at the crack tip. In the case of isotropic, homogeneous, ductile materials, a plastic zone is observed. The length of the zone, r_p , can be

estimated from the expression [21]

$$r_p = \frac{G_1 E}{2\pi\sigma_y^2}$$

where G_1 is the strain-energy release rate, which for a crack which is stressed sufficiently to propagate, is equal to twice the fracture surface energy. E is the modulus, and σ_y the tensile flow stress (or yield stress) of the material. The zone is usually treated as being of approximately circular section, having radius r_p .

Similar stress concentrations occur in non-isotropic materials, and expressions for stresses have been derived for the orthotropic case, which includes aligned fibre composites [22]. The stresses fall off with distance from the crack, r , as $r^{-1/2}$, which is exactly the same decrease obtained with isotropic materials. However, the variation of stress with angle of the radius vector to the crack plane is different, and so is the effective modulus. Thus in the orthotropic case, the zone of very high stress will have a different shape and cross-sectional area from that in the isotropic case.

For sufficiently sharp cracks, under sufficiently high stresses, a finite zone should exist in which the strength of the composite is exceeded. If the breaking strain of the fibres is less than that of the matrix, and if the zone is sufficiently extensive in the fibre direction, brittle fibres could break up into lengths of between $l_c/2$ and l_c [14]. Let the length of the zone in the fibre direction be

$$r_p = \frac{a\gamma E_{\text{eff}}}{\pi\sigma_{cu}^2} \quad (15)$$

where a is a geometrical constant resulting from orthotropy. (a will probably have to be measured experimentally, since it is very difficult to calculate the size and shape of the plastic zone, even in isotropic homogeneous materials.) E_{eff} is the effective modulus [7], and σ_{cu} is the ultimate tensile strength of the composite.

When the ratio of fibre and matrix moduli is greater than 10, E_{eff} is given with sufficient accuracy (see Halpin and Tsai [23], and compare with Goggin [24]), by

$$E_{\text{eff}} \simeq 5V_f \sqrt{G_m E_f} \quad (16)$$

where G_m is the shear modulus of the matrix. For $V_f \geq 0.1$ for strong fibres in a weak matrix,

$$\sigma_{cu} \simeq V_f \sigma_{fu} \quad (17)$$

If pull-out occurs, γ is given by Equation 2 with $s \simeq 3s_c/4$, i.e.

$$\gamma \approx \frac{1}{12} V_f d \tau_i s_e^2. \quad (18)$$

Substituting Equations 16, 17 and 18 into Equation 15 gives

$$r_p \approx \frac{ad\tau_i s_e^2 \sqrt{(G_m E_f)}}{15\sigma_{fu}^2}.$$

But for fibre break-up to occur, $r_p > l_c$. Thus for fibre break-up we have the condition

$$\frac{30\sigma_{fu}}{\sqrt{(G_m E_f)}} < a \quad (19)$$

or for fibres and matrix having about the same elastic constants

$$\frac{150V_f \sigma_{fu}}{E_f} < a. \quad (19a)$$

Without a knowledge of the value of a , we can only put the materials discussed herein in order of decreasing likelihood of pull-out effects for initially continuous fibres. This is as follows, the values in brackets being the approximate sizes of the left hand side of Equation 19 or 19a.

- carbon in glass (0.52), pull-out most likely;
- carbon in epoxy (2.3);
- boron in epoxy (3.6);
- glass in epoxy (5.1), pull-out least likely.

Note that neither condition contains τ_i . Thus, drastically reducing τ_i , as for example has been done by Harris and co-workers [25], should not change the fracture process from fibre pull-out to fibre fracture in the crack plane.

4. Conclusions

The dependence of fracture energy on aspect ratio appears to be far from straightforward. Three distinct types of behaviour can be recognized; which category a material belongs to depends mainly on the fibre properties and, to a lesser extent, on matrix properties. The dominant property is the fibre ductility, and the three cases may be listed in order of decreasing fibre ductility as follows:

1. ductile fibres which dissipate a large amount of internal energy when they fracture. Composites containing these fibres should be made with very long fibres, to maximize the fibres' contribution to the work of fracture;
2. brittle fibres and moderately ductile fibres having uniform strength. Pull-out effects will give maximum toughness with these fibres, and to achieve moderate toughness the fibre length

should not be greater than about ten times the critical length for reinforcement. (The fibre length cannot be very much less than this value without unduly decreasing stiffness and modulus);

3. brittle fibres having flaws. The behaviour of composites containing these fibres depends on the value of the ratio $\sigma_{fu}/\sqrt{(E_f G_m)}$ (or $V_f \sigma_{fu}/E_f$ when the elastic properties of fibres and matrix are nearly the same). Low values of this ratio indicate that pull-out effects can occur with continuous fibres. Thus for these cases (e.g. carbon fibres in epoxy resins) continuous or very long fibres should be used. For composites having high values of the ratio, the fibres should have aspect ratios of about ten times the critical (or somewhat less than this if a significant loss in strength and stiffness is acceptable).

The fibre diameter affects the toughness in the moderately ductile, and brittle fibre cases. In these cases, the fibre diameter should be as large as possible to maximize toughness. Doing this by using reinforcing rods made from impregnated fibre bundles, however, could transfer a material from category 3 to category 2, and so may not always be advantageous.

Acknowledgements

The author is indebted to many workers in the field with whom he has had private discussions, and in particular to Dr A Wronski for pointing out the effect thin fibres can have on ductile matrices, and Dr B. Harris for directing his attention to the fibre break-up that can occur in the highly stressed regions at crack tips.

References

1. A. WRONSKI (private communication).
2. J. L. HELFET and B. HARRIS, *J. Mater. Sci.* **7** (1972) 494
3. W. W. GERBERICH, *ibid* **5** (1970) 283.
4. J. COOK and J. E. GORDON, *Proc. Roy. Soc. (Lond.)* **A282** (1964) 508.
5. G. A. COOPER and A. KELLY, *J. Mech. Phys. Solids* **15** (1967) 279.
6. G. A. COOPER, *J. Mater. Sci.* **5** (1970) 645.
7. P. W. BEAUMONT and B. HARRIS, *ibid* **7** (1972) 1265.
8. D. C. PHILLIPS, *ibid* **7** (1972) 1175.
9. J. OUTWATER and M. MURPHY, 24th Ann. Conf. Soc. Plas. Ind. Section 11c (1969) pp. 1-7.
10. M. R. PIGGOTT, *J. Mater. Sci.* **5** (1970) 669.
11. J. F. MANDELL and F. J. MCGARRY, M.I.T. Dept. of Civil Eng., Report R72-11 (1972).
12. M. FILA, C. BREDIN and M. R. PIGGOTT, *J. Mater. Sci.* **7** (1972) 983.
13. P. HING and G. W. GROVES, *ibid* **7** (1972) 427.
14. A. KELLY and G. DAVIES, *Metall. Rev.* **10** (1965) 1.

15. S. FLOREEN, H. W. HAYDEN and R. M. PILLIAR, *Trans. Met. Soc. AIME* **245** (1969) 2569.
16. M. R. PIGGOTT, *J. Mech. Phys. Solids* (1974) to be published.
17. R. E. ALLRED and D. M. SCHUSTER, *J. Mater. Sci.* **8** (1973) 245.
18. D. M. SCHUSTER and E. SCALA, "Fundamental Aspects of Fibre Reinforced Plastic Composites" (edited by Schwartz and Schwartz) (Wiley, New York, 1968) p. 45.
19. R. A. SAMBELL, A. BRIGGS, D. PHILLIPS and D. BOWEN, *J. Mater. Sci.* **7** (1972) 676.
20. R. A. SAMBELL, D. H. BOWEN and D. C. PHILLIPS, *ibid* **7** (1972) 663.
21. V. WEISS and S. YUKAWA, ASTM STP 381 (1964) p. 1.
22. G. C. SIH, P. C. PARIS and G. R. IRWIN, *Int. J. Fract. Mech.* **1** (1965) 189.
23. J. C. HALPIN and S. W. TSAI, AFML TR67-423 (1969).
24. P. R. GOGGIN, *J. Mater. Sci.* **8** (1973) 233.
25. B. HARRIS, P. W. BEAUMONT and E. MONCUNILL DE FERRAN, *J. Mater. Sci.* **6** (1971) 238.

Received 27 February and accepted 31 July 1973.